Research Article | Vol. 29, No. 23 / 8 Nov 2021 / Optics Express 37429
Optics EXPRESS

Timing and X-ray pulse characterization at the Small Quantum Systems instrument of the European X-ray Free Electron Laser

PATRIK GRYCHTOL,[1,7] DANIEL E. RIVAS,[1] THOMAS M. BAUMANN,[1] REBECCA BOLL,[1] ALBERTO DE FANIS,[1] BENJAMIN ERK,[2] MARKUS ILCHEN,[1,3] JIA LIU,[1] TOMMASO MAZZA,[1] JACOBO MONTAÑO,[1] JOST MÜLLER,[2] VALERIJA MUSIC,[1,3] YEVHENIY OVCHARENKO,[1] NILS RENNHACK,[1] ARNAUD ROUZÉE,[4] PHILIPP SCHMIDT,[1] SEBASTIAN SCHULZ,[2] SERGEY USENKO,[1] RENÉ WAGNER,[1] PAWEL ZIOŁKOWSKI,[1] HOLGER SCHLARB,[2] JAN GRÜNERT,[1] NIKOLAY KABACHNIK,[1,5,6] AND MICHAEL MEYER[1,8]

[1]*European XFEL, Holzkoppel 4, 22869 Schenefeld, Germany*
[2]*Deutsches Elektronen-Synchrotron DESY, Notkestrasse 85, 22607 Hamburg, Germany*
[3]*University of Kassel, Department of Physics, Heinrich-Plett-Straße 40, 34132 Kassel, Germany*
[4]*Max-Born-Institut, Max-Born-Straße 2A, 12489 Berlin, Germany*
[5]*Donostia International Physics Center, Paseo Manuel de Lardizabal 4, E-20018 San Sebastian, Spain*
[6]*Skobeltsyn Institute of Nuclear Physics, Lomonosov Moscow State University, Moscow 119991, Russia*
[7]*grychtol@xfel.eu*
[8]*michael.meyer@xfel.eu*

Abstract: This contribution presents the initial characterization of the pump-probe performance at the Small Quantum Systems (SQS) instrument of the European X-ray Free Electron Laser. It is demonstrated that time-resolved experiments can be performed by measuring the X-ray/optical cross-correlation exploiting the laser-assisted Auger decay in neon. Applying time-of-arrival corrections based on simultaneous spectral encoding measurements allow us to significantly improve the temporal resolution of this experiment. These results pave the way for ultrafast pump-probe investigations of gaseous media at the SQS instrument combining intense and tunable soft X-rays with versatile optical laser capabilities.

1. Introduction

The advent of highly brilliant X-ray free electron laser facilities reaching photon energies of several thousand of electron volts (eV) has opened up intriguing possibilities to study atoms, molecules and bulk matter [1]. Their energy-tunable, ultra-short and partially coherent photon pulses allow for site-specific investigations of light-matter interactions on the natural time scales of the fundamental nuclear as well as electronic motion in unprecedented detail [2,3]. To this end, time-resolved experiments have commonly favored a pump-probe approach, in which the reaction of a system is triggered by a *pump* pulse, while its subsequent evolution is monitored by a temporally shifted *probe* pulse. Especially if these pulses are derived from different and independently operating sources, such as an accelerator-based X-ray free electron laser (XFEL) and an optical laser (OL), the temporal resolution of any measurement is not only limited by the duration of the respective pulses, but also depends on the timing jitter between them. Thus, for conducting pump-probe experiments with the highest possible time resolution, it is of

#440718 https://doi.org/10.1364/OE.440718
Journal © 2021 Received 17 Aug 2021; revised 27 Sep 2021; accepted 6 Oct 2021; published 27 Oct 2021

Optics EXPRESS

utmost importance to accurately synchronize the different light sources and to compensate any residual jitter.

The synchronization of an OL and an XFEL is generally accomplished by stabilizing the pulse train of the OL seed oscillator with respect to the radio frequency (RF) driving the electron bunches in the XFEL accelerator. Thereby, a relative timing jitter in the range of a few tens to a few hundred femtoseconds can be achieved [4–9]. This can be further reduced to the sub-10 fs level using a dedicated balanced optical cross-correlation technique based on the actively stabilized distribution of an optical reference signal [10]. A significant portion of the remaining jitter originates from thermal and mechanical fluctuations and electronic drifts of individual accelerator components as well as from the self-amplified spontaneous emission (SASE) process generating X-rays in the undulator section [6,11–13]. To overcome these inherent shortcomings, the most practical approach is to measure the relative arrival time of the pump and probe pulses on a single shot basis and sort the data accordingly in the subsequent analysis process [14–24], potentially achieving sub-femtosecond accuracy [25]. A more advanced but rather challenging technique to minimize the timing jitter is to seed a free electron laser [26].

In the following, this contribution presents a first characterization of the pump-probe capabilities at the Small Quantum Systems (SQS) instrument of the European XFEL [27,28]. This recently commissioned instrument is dedicated to investigations of atoms, ions, molecules and clusters in intense laser fields, including studies of non-linear phenomena and the dynamics of photo-induced processes. The present work serves as a benchmark experiment, both to quantify its current timing performance and to provide an initial characterization of the X-ray pulse duration at the European XFEL. For this purpose, timing diagnostics based on spectral encoding were used to monitor the relative arrival time between the XFEL and synchronized OL pulses [29,30]. These measurements revealed a relative timing jitter of approximately 58 fs ± 1 fs (FWHM) under the described conditions. This result is comparable to other instruments and XFEL facilities around the world [4–9]. In addition, an X-ray/optical cross-correlation was measured, exploiting the laser assisted Auger decay in neon [31,32] revealing an upper limit of the average XFEL pulse length of 38 ± 2 fs (FWHM). Thus, the feasibility of conducting pump-probe experiments with active time-of-arrival sorting was demonstrated. These results constitute the first investigation of the pump-probe capabilities at the SQS instrument and they simultaneously provide an initial assessment of the X-ray pulse duration at the European XFEL, which is representative of the operation conditions at the time of the experiment.

2. Experiment

The SQS scientific instrument is designed for investigations of atomic and molecular systems, as well as clusters, nano-particles and small bio-molecules [33–37]. It is located about 450 m downstream of the SASE 3 undulator, which emits horizontally polarized radiation in a photon energy range between 260 eV and 3000 eV (4.8 nm to 0.4 nm) exceeding 10^{12} photons per pulse and delivering up to 27000 pulses per second in a 10 Hz bunch pattern mode [27]. Two elliptical mirrors in Kirkpatrick-Baez configuration can focus the XFEL beam to a spot size of about 1 μm in diameter (FWHM). For this study a photon energy of 1000 eV was chosen, at which a pulse energy of up to 5 mJ was obtained. This resulted in an intensity of more than 10^{18} W/cm^2 at the focus, where the Atomic-like Quantum Systems (AQS) chamber was centered around to measure the X-ray/optical cross-correlation (see Fig. 1). The timing jitter was measured by a Photon Arrival time Monitor (PAM) [30] mounted about 1.8 m downstream, where the X-ray spot has already diverged to a diameter of around 1.5 mm (FWHM).

For this investigation, a fiber-based OL system was used, which delivered sub-300 fs pulses with an energy of up to 2 mJ at a central wavelength of 1030 nm. These pulses were compressed by a hollow core fiber providing sub-40 fs laser pulses with a conversion efficiency of more than 50 % at a repetition rate of 112 kHz. A typical OL (reference) spectrum and an intensity

Optics EXPRESS

auto-correlation measurement with a FWHM of about 54 fs deconvolving to a OL pulse length of 38.1 ± 0.2 fs are shown in Fig. 2. The pulse-picking acousto-optic-modulator of the OL amplifier system was used to mimic the 10 Hz XFEL bunch structure. The OL seed oscillator was synchronized to a pulsed optical reference by means of a balanced optical cross-correlator resulting in an in-loop jitter of less than 10 fs (root-mean-square). This optical reference was stabilized to the master RF clock of the European XFEL and it was delivered to the OL using length-stabilized optical fiber links ensuring the precise synchronization of the OL with regard to the X-ray pulse train [38].

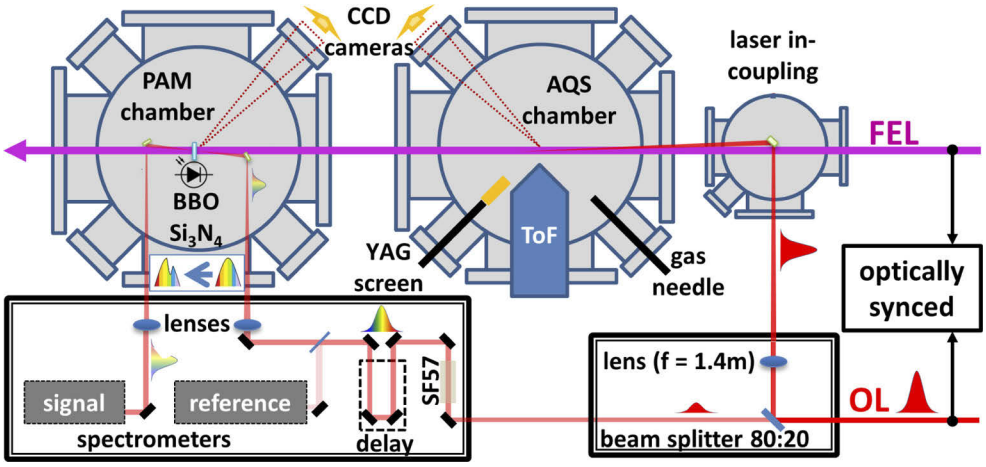

Fig. 1. Schematics of the experimental setup and the laser beam paths: The XFEL pulses are focused into the AQS chamber, where the X-ray/optical cross-correlation is measured. Thereafter, they propagate into the PAM chamber for measurements of their relative arrival times with respect to the synchronized OL pulses.

Before entering the vacuum chambers, the OL beam was split into two beams with a ratio of 80:20 (see Fig. 1). For the X-ray/optical cross-correlation measurement, the intense portion of the OL beam was focused with a lens (f = 1.4 m) into the AQS chamber propagating nearly co-linearly (<0.5°) to the X-ray beam. Its focused beam waist diameter was determined to be around 200 μm (FWHM), which allowed for delivering a peak intensity of more than 10^{14} W/cm^2 on target. The two orders of magnitude larger OL focus with respect to the soft X-ray spot size ensured the two-color experiment to be insensitive to any pointing instabilities. The spatial overlap of the XFEL and OL beams was established on a Cerium doped Yttrium Aluminum Garnet (YAG) screen, which could be inserted into the interaction zone. A fast photo-diode (Hamamatsu G4176) in combination with a 12.5 GHz oscilloscope (Tektronix DPO71254C) was first used to narrow down the temporal overlap to less than 100 ps. Applying the spectral encoding technique in the PAM allowed for pinpointing the temporal overlap into the femtosecond regime, after balancing both laser arms by means of the second harmonic signal generated in a β−Barium Borate (BBO) crystal located in the PAM.

For the timing characterization, the weaker portion of the OL beam was directed to the PAM, where it first passed through a 300 mm long SF57 glass rod stretching the optical pulse to about 3 ps. Thereafter, it was sent to a motorized delay stage, downstream of which a small amount was leaked into a (reference) spectrometer (Ocean Optics HDX-XR). After the delay stage, the OL beam was lead into the PAM chamber and focused onto a 1 μm thin Si_3N_4 membrane, which was also illuminated by the mm-sized soft X-ray beam from the AQS chamber. The XFEL pump pulse changed the refractive index and thus transmission of the membrane material. This transient response was probed by the chirped optical pulse such that the relative delay to the

Optics EXPRESS

soft X-ray pulse was mapped onto the optical laser spectrum, a technique known as spectral encoding [29]. This spectrum was simultaneously recorded by another (signal) spectrometer (Ocean Optics HDX-XR) located outside the PAM chamber.

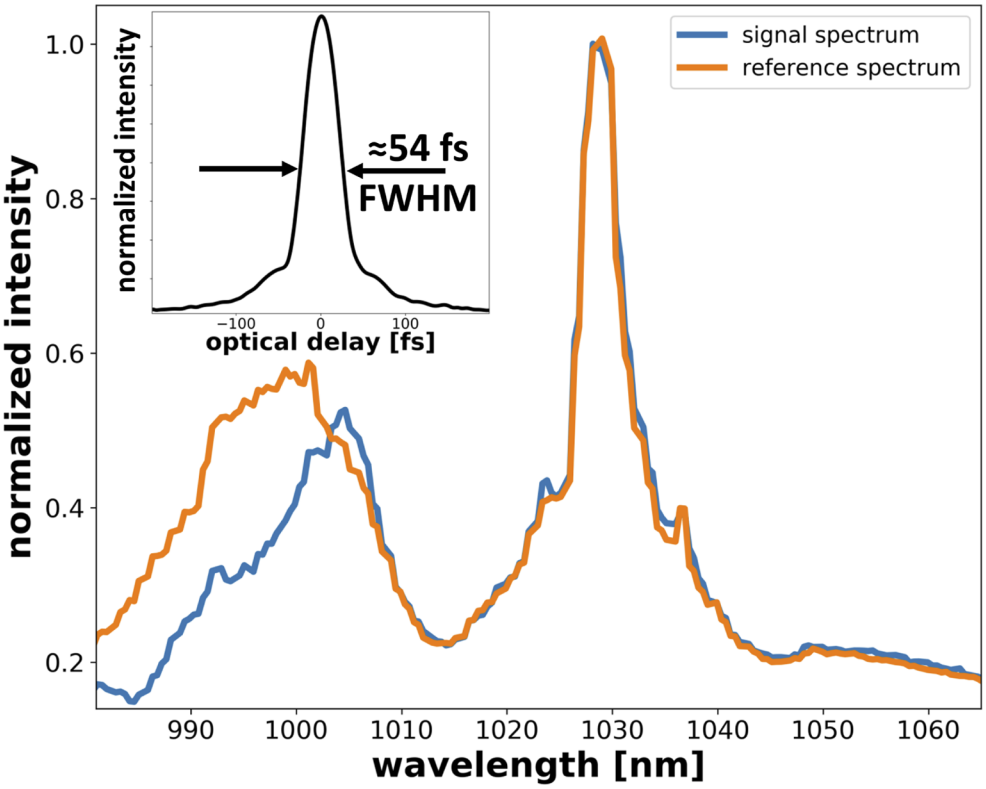

Fig. 2. Typical single-shot spectra of the chirped OL pulse before (reference) and after (signal) passing through a 1 μm thin Si_3N_4 membrane at XFEL/OL overlap, leading to a change in transmission around 1000 nm. An intensity auto-correlation of the OL with a FWHM of about 54 fs is shown in the inset. It results in a pulse length of 38.1 ± 0.2 fs, as determined by a Gaussian fit to the numerical deconvolution of this measurement.

2.1. Monitoring pulse arrival times

For every single XFEL/OL pulse, two optical spectra were recorded (signal and reference) to account for shot-to-shot spectral intensity fluctuations. Typical spectra, which have also been normalized by the response function of the sample, are displayed in the main graph of Fig. 2. For this particular shot, the impact of the XFEL pulse on the Si_3N_4 membrane is clearly visible as a significant reduction in the transmitted intensity of the signal spectrum around 1000 nm when compared to the reference spectrum. In order to map the wavelength onto a time axis and to quantify the timing jitter, the PAM was first calibrated by recording OL transmission spectra as a function of the XFEL (pump) and OL (probe) time delay, which was varied in a controlled manner using a motorized delay stage placed in the OL beam path. For each time delay, a total of about 100 pairs of spectra were recorded and for each pair, the relative wavelength (λ) dependent change in optical transmission was evaluated, using $\Delta T(\lambda) = S_{sig}(\lambda)/S_{ref}(\lambda) - 1$, with $S_{sig}(\lambda)$ and $S_{ref}(\lambda)$ defined as the normalized spectral intensities of the signal and reference spectra, respectively.

Optics EXPRESS

As displayed in the inset of Fig. 3, the resulting change in transmission resembles a step-like function, which was fitted with an error function to extract the spectral positions encoding the relative arrival time of an XFEL pulse with respect to an OL pulse. The result of this procedure is shown in the main graph of Fig. 3, as a function of the time delay in steps of 10 fs set by the motorized delay stage. While there is a substantial fluctuation of the spectral position retrieved for each time delay due to the inherent timing jitter between the OL and the XFEL pulses, the average spectral position linearly increases with increasing time delay. Using a linear regression, a wavelength or pixel to time conversion of 32.9 ± 0.6 fs/nm or 13.8 ± 0.3 fs/pixel was extracted, respectively. Harmand et al. concluded that the error bars obtained from the fitting procedure are a good measure of the uncertainty in determining the relative arrival time between OL and XFEL pulses using a single timing diagnostic [18]. On a single shot basis, Gaussian error propagation revealed that the overall error of the fitting procedure to the calibration data averages to a value of about 7 fs (FWHM), which can be neglected with respect to other involved time scales.

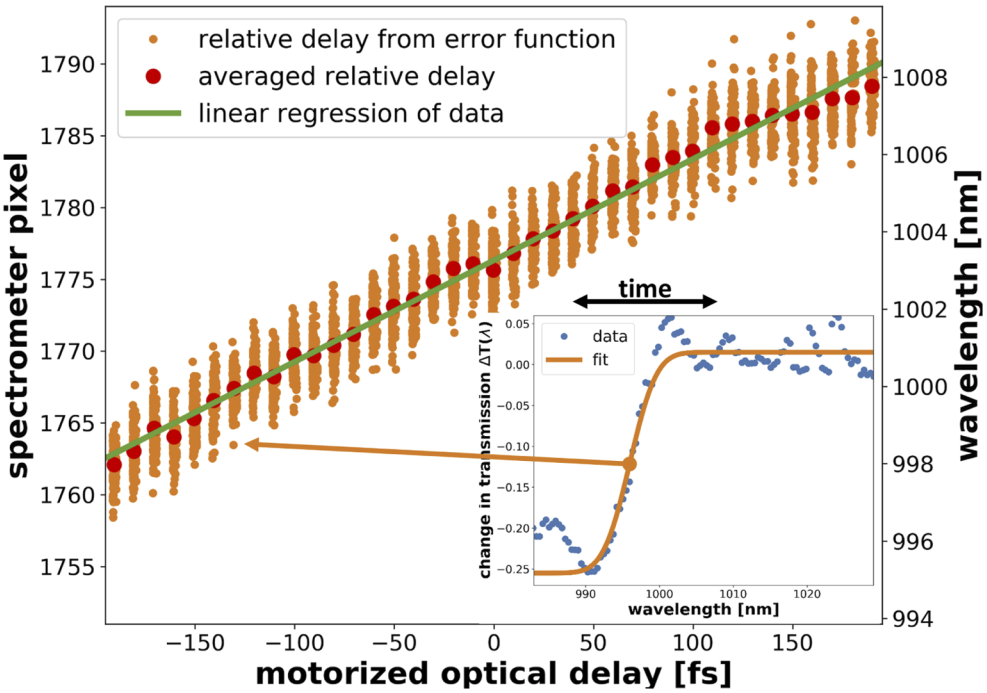

Fig. 3. The inset shows the typical change in transmission $\Delta T(\lambda)$ of a 1 μm thin Si_3N_4 membrane due to OL/XFEL overlap (blue dots) and a corresponding error function fit (orange line), whose central slope position represents the relative arrival time between XFEL and OL pulses. The main graph shows the extracted slope positions (orange dots), about 100 per 10 fs optical delay step, and a corresponding linear fit (green line).

Following the calibration of the PAM, the timing jitter was then determined by evaluating about 4000 single shot pairs of spectra recorded at a fixed position of the motorized delay stage and acquired at a repetition rate of 10 Hz. The relative arrival time between the XFEL and OL extracted from each individual pulse is displayed in Fig. 4, showing a jitter of 58 ± 1 fs (FWHM). This compares well with results from other instruments at the European XFEL [8,9] as well as other XFEL facilities around the world [4–7]. However, it is important to note that when sorting single shots in accordance to their measured time-of-arrival, it is possible to improve the temporal resolution of the experiments to values well below the measured jitter, as shown in the following. This approach is ultimately limited by the experimental uncertainty of the PAM in

Optics EXPRESS

combination with the mechanical stability of the entire experimental setup and other possible sources of systematic errors. Investigations at other facilities and at European XFEL show typical relative uncertainty values at the order of 10 fs - 15 fs (FWHM) [18,39].

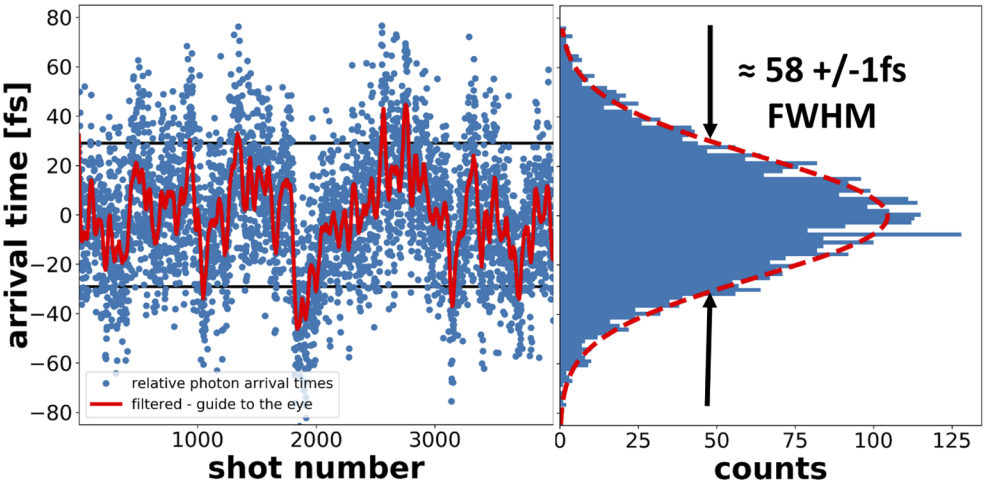

Fig. 4. Single shot timing jitter between OL and XFEL retrieved from the photon arrival time monitor based on spectral encoding (left) and the corresponding histogram (right). A Gaussian fit (red dashed line) allows for extracting a jitter of 58 ± 1 fs (FWHM).

These results can be improved even further when the spectral resolution of the spectrometer is increased and/or the chirp of the OL pulse in the PAM is tailored to the experimental requirements. Moreover, it is important to also identify, properly characterize and eventually mitigate major physical sources of the timing jitter caused by a variety of effects, such as vibrations of individual instrument components along the nearly 30 m long OL beam path, temperature and humidity instabilities in the SQS experimental hutch. In addition, there are ongoing efforts to improve the stability of the electron bunch structure in the accelerator sections of the European XFEL, thereby also reducing undesired temporal fluctuations of the X-ray pulse train [40].

2.2. *Measuring X-ray/optical cross-correlation*

Having characterised the timing jitter at the SQS instrument, the X-ray/optical cross-correlation experiment was subsequently conducted in the AQS chamber by simultaneously monitoring the relative pulse arrival times as specified above. For this purpose, electron spectra from laser assisted Auger decay in neon were recorded at 10 Hz, as a function of the time delay between the optical laser pulses centered at 1030 nm (1.2 eV) and the soft X-ray pulses tuned to 1 keV (1.24 nm). The XFEL photons generated an Auger electron distribution dominated by the transition between the states $Ne^{+}1s^{-1}2p^{6}$ and $Ne^{2+}2p^{4}\,{}^{1}D_{2}$ yielding a characteristic kinetic electron energy of 804.3 eV [41]. In the presence of the intense OL field, these electrons were dressed along its polarization axis, changing their kinetic energy and thereby giving rise to a characteristic sideband structure [42–45]. These sidebands were separated by the OL photon energy due to the absorption or emission of 1.2 eV photons by the X-ray generated Auger electrons. Being a two-color generated signal, the intensity of the sidebands constitutes a higher order cross-correlation of the OL and XFEL pulses [31].

The electron spectra were measured by the time-of-flight (ToF) spectrometer of the AQS chamber located in the horizontal polarization plane of the XFEL/OL laser pulses [46]. This custom made spectrometer was specifically designed to record electron spectra at MHz repetition rates and a resolving power ($E/\Delta E$) exceeding 10,000 has been demonstrated at a synchrotron

Optics EXPRESS

radiation source. In combination with intense XFEL pulses a resolution of about 0.5 eV at a kinetic energy of 800 eV was achieved up to now. Neon was introduced in the AQS chamber by means of a needle moved close to the interaction region. Under gas load the background pressure increased to $2 \cdot 10^{-7}$ mbar, while the target density in the interaction region was estimated to be one to two orders of magnitude higher. The FEL intensity was kept at 10^{18} W/cm^2, and the intensity of the OL was deliberately attenuated to about $5 \cdot 10^{10}$ W/cm^2 keeping the sideband order low to ease the interpretation of the sideband spectra displayed in Fig. 5. The left graph of this figure shows the result of the measurement based on sorting the spectra with respect to the delay stage position only, whereas the electron spectra displayed in the right graph have been sorted according to the extracted relative pulse arrival times with a binning of 10 fs and 5 fs, respectively. Both graphs show that at large as well as small pump-probe delays the spectra are dominated by the single Ne (1s) Auger electron peak. As the delays approach time zero, the distinct Auger line starts to vanish while equally spaced sidebands up to the third order appear, both at lower and higher electron energies.

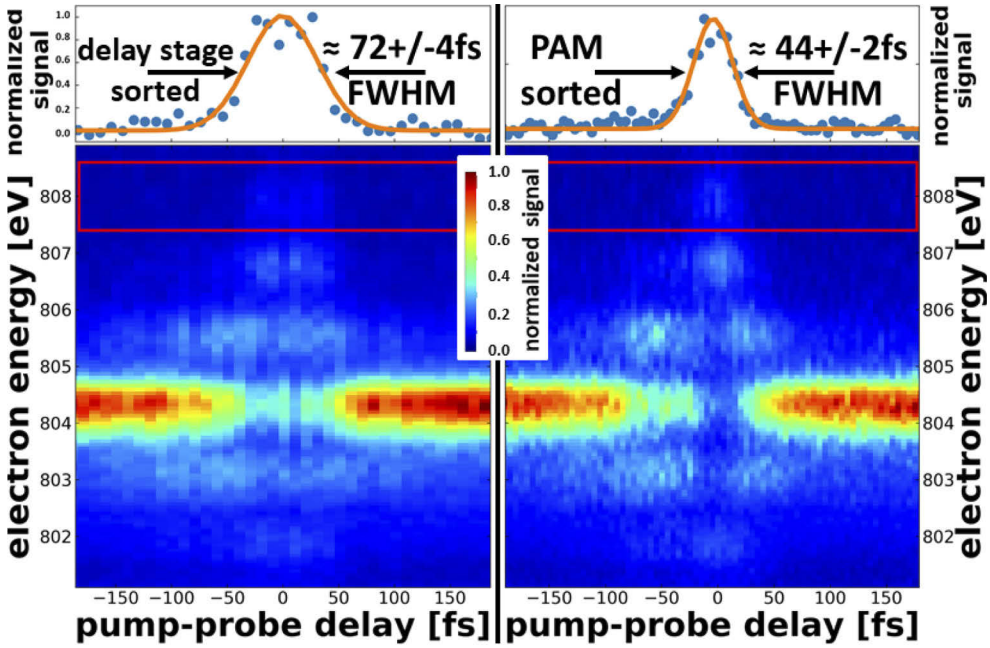

Fig. 5. X-ray/optical cross-correlation measurement results: Electron spectra from laser-assisted Auger decay in neon, as a function of the time delay between the XFEL (pump) and the OL (probe); spectra sorted according to the delay stage position on the left and PAM-sorted spectra on the right for which about 50 to 120 spectra per step have been averaged. The top graphs show the normalized integral (blue dots) from the region marked by the red boxes including Gaussian fits (orange lines).

3. Results and discussion

By comparing both graphs in Fig. 5, it can be clearly seen that sorting the time-dependent electron spectra using the results from the PAM allows for improving the time resolution below the jitter level. In particular, a distinct depletion of the electron signal in the main Auger line as well as the first order sideband appears at time zero. To evaluate the cross-correlation and to estimate the improvement, the electron signals recorded in the energy ranges from 807.4 eV to 808.4 eV (see red boxes in the graphs), corresponding to the third sideband order, were integrated,

Optics EXPRESS

normalized by amplitude and fitted with Gaussian functions (see top graphs in Fig. 5). The third and highest order sidebands have been chosen because they are not affected by any depletion effects related to intracycle electron interference in this non-pertubative intensity regime [43,47]. This analysis yields cross-correlation FWHM of τ_{CC}= 72 ± 4 fs for the delay stage sorted data and τ_{CC}= 44 ± 2 fs for the PAM sorted data. In order to assess the XFEL pulse duration τ_{XFEL} from this measurement result, the following, easily derived analytical expression assuming the convolution of three Gaussian pulses was used [47]:

$$\tau_{XFEL} = (\tau_{CC}^2 - \tau_{OL}^2/n - \tau_{EXP}^2)^{1/2}, \quad (1)$$

with n accounting for the order of the involved non-linearity in the cross correlation measurement. Considering an OL pulse length of τ_{OL}= 38.1 ± 0.2 fs (see inset in Fig. 2) and disregarding the experimental uncertainty (τ_{EXP} = 0), it is possible to provide an upper limit for the X-ray pulse length. Having selected the third sideband order and neglecting the nearly instantaneous Auger process (≈ 2.4 fs), the ceiling of the average X-ray pulse length is calculated to be 38 ± 2 fs. On the other hand, if a typical sorting accuracy, i.e. experimental uncertainty of $\tau_{EXP} = 15\,fs$ is assumed as discussed above, a XFEL pulse duration of $\tau_{XFEL} \approx$ 35 ± 2 fs can be inferred. This value is quite close to the upper limit and it can be concluded that the cross-correlation signal and consequently the temporal resolution of the SQS instrument was dominated by the duration of the XFEL pulses when the experimental data is sorted according to the PAM measured time-of-arrival, as the effective OL pulse duration amounts to $(38^2/3)^{1/2} \approx 22\,fs$ for the third sideband. It should be noted however that the calculated numbers were deduced for the operation configuration at the time of the measurement when the accelerator was filled with a bunch charge of 250 pC at an electron energy of 14 GeV. More recent measurements suggest that the pulse duration can be shorter for other settings of the European XFEL.

3.1. TDSE simulations

In order to support the analysis of the X-ray/optical cross-correlation measurement, the sideband experiment has been simulated using a theoretical approach [48], the result of which is displayed in Fig. 6. It is based on an approximate solution of the time dependent Schrödinger equation (TDSE) describing the excitation and the decay of the Auger state in the dressing OL field within the strong field approximation. In the simulation, an OL pulse length of 38 fs (FWHM) and an XFEL pulse length of 35 fs (FWHM) were assumed. The intensities of the two pulses were set to match the experimental values. To account for the experimental uncertainty τ_{EXP}, the result was additionally convolved by a Gaussian function with a FWHM of 15 fs. Both from a qualitative and a quantitative point of view, the simulations agree well with the experimental time-resolved spectra. A maximum of three to four sideband orders are visible in both cases. Moreover, the depletion of the Auger line and the first sideband order due to intracycle interference can be reproduced [43]; see line-out indicated by the white dashed line taken at 805.5 eV from the intensity graph in Fig. 6. On the other hand, the experimental spectra appear less symmetric than the simulated spectra. Additional SIMION simulations confirm that the asymmetry in kinetic energy with respect to the Auger line is due to the energy dependent transmission of the electron ToF spectrometer [46,49]. The horizontal asymmetry with respect to the time zero axis are attributed to the non-Gaussian nature of the OL pulse (see inset in Fig. 2). For a quantitative comparison, the time-dependent electron signal calculated at a photon energy of 807.9 eV has been normalized and displayed at the top of Fig. 6 (indicated by a white dashed line in the adjacent intensity graph). A fit with a Gaussian function to this third order sideband signal yields a cross-correlation FWHM of τ_{CCsim}= 42.6 ± 0.1 fs, which basically confirms the experimental findings.

Optics EXPRESS

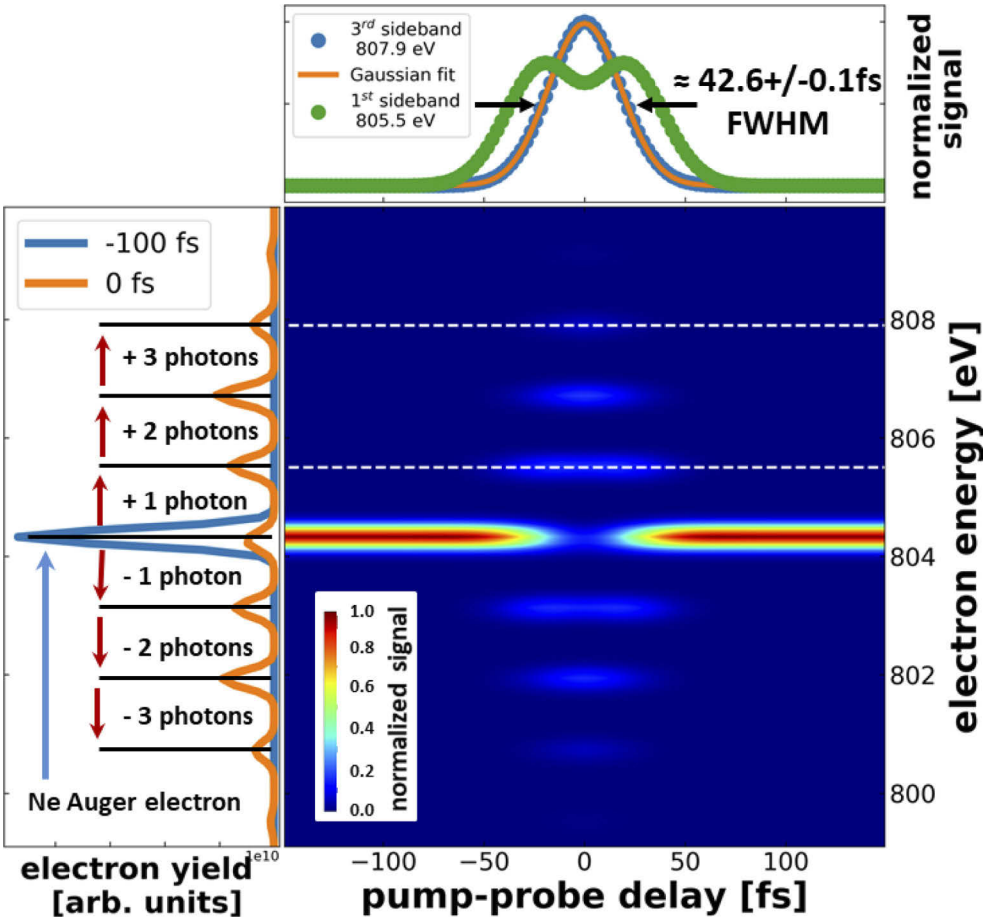

Fig. 6. TDSE based simulations of electron spectra from laser-assisted Auger decay in neon, as a function of the time delay between the XFEL ($1 \cdot 10^{18}$ W/cm^2 - 35 fs) and the OL ($5 \cdot 10^{10}$ W/cm^2 - 38 fs) pulses considering a temporal uncertainty of 15 fs (FWHM). The top graph shows line-outs of the first (green dots - 805.5 eV) and third (blue dots - 807.9 eV) order sidebands (see white dashed lines), including a Gaussian fit (orange line) to the latter resulting in a cross-correlation FWHM of τ_{CCsim}= 42.6 ± 0.1 fs. The graph on the left shows electron spectra for two time delays between the OL and the XFEL pulses.

Optics EXPRESS

4. Conclusion

The results of this measurement represent the first study of the timing performance and an initial X-ray pulse length characterization at the Small Quantum Systems instrument of the European XFEL. This study successfully demonstrates the feasibility of conducting pump-probe experiments at the SQS instrument in combination with utilizing the installed photon arrival time monitor based on spectral encoding. The measurement of the relative arrival times between the XFEL and the synchronized optical laser pulses resulted in a timing jitter of 58 ± 1 fs (FWHM). By using the aforementioned timing diagnostics in a time-resolved two-color sideband experiment, a third order X-ray/optical cross-correlation allowed for determining an upper limit of the average soft X-ray pulse length of 38 ± 2 fs (FWHM) at the given operation condition of the XFEL. Assuming a typical sorting accuracy of 15 fs, this limit can be narrowed down to 35 ± 2 fs suggesting that the temporal resolution of the experiment was mainly limited by the pulse duration of the X-rays, thereby providing plenty of room for improvements. These results are supported by corresponding TDSE simulations and provide the first assessment of the X-ray pulse duration at the European XFEL.

It is important to note that there are continuous efforts at all levels of the European XFEL facility to constantly improve its overall performance. For example, the electron beam side works on controlling the XFEL pulse duration and its temporal structure, which will greatly benefit from the electron bunch arrival monitors that were under commissioning and not fully operational during this experiment [40,50,51]. More recent measurements suggest that the pulse duration can be shortened for other settings of the XFEL. Besides the identification as well as the reduction of a variety of jitter sources, next steps at the SQS instrument include the commissioning of the PAM at MHz repetition rates [9] and the deployment of the dedicated pump-probe laser at SASE 3, already delivering few mJ pulses with a duration of 15 fs [52,53]. Moreover, the spectral range of the femtosecond laser infrastructure is currently extended into the infrared as well as extreme ultraviolet region. Overall, this work paves the way for ultrafast pump-probe investigations of gaseous media at the SQS instrument combining intense and tunable soft X-rays with versatile optical laser capabilities.

Acknowledgments. The authors acknowledge the European XFEL in Schenefeld, Germany, for providing X-ray Free-Electron Laser beamtime at the SQS instrument and thank the staff for its relentless effort and assistance around the clock. The SQS group appreciates the design of the photon arrival time monitor by the X-ray Photon Diagnostics (XPD) group of the European XFEL. MM, TM, and RW acknowledge support by the Deutsche Forschungsgemeinschaft (DFG, German Research Foundation) – SFB-925 – project 170620586. MI and VM are thankful for the financial support of the Peter Paul Ewald fellowship by the Volkswagenstiftung. NK acknowledges the hospitality and the financial support from the theory group of the European XFEL and the Donostia International Physics Center.

Disclosures. The authors declare no conflicts of interest.

Data availability. Data underlying the results presented in this paper are available in Ref. [54].

References

1. B. McNeil and N. Thompson, "X-ray free-electron lasers," Nat. Photonics **4**(12), 814–821 (2010).
2. J. Feldhaus, M. Krikunova, M. Meyer, T. Möller, R. Moshammer, A. Rudenko, T. Tschentscher, and J. Ullrich, "AMO science at the FLASH and European XFEL free-electron laser facilities," J. Phys. B: At. Mol. Opt. Phys. **46**(16), 164002 (2013).
3. C. Bostedt, S. Boutet, D. Fritz, Z. Huang, H. Lee, H. Lemke, A. Robert, W. Schlotter, J. Turner, and G. Williams, "Linac Coherent Light Source: The first five years," Rev. Mod. Phys. **88**(1), 015007 (2016).
4. J. Glownia, J. Cryan, J. Andreasson, A. Belkacem, N. Berrah, C. I. Blaga, C. Bostedt, J. Bozek, L. F. DiMauro, L. Fang, J. Frisch, O. Gessner, M. Gühr, J. Hajdu, M. P. Hertlein, M. Hoener, G. Huang, O. Kornilov, J. P. Marangos, A. M. March, B. K. McFarland, H. Merdji, V. S. Petrovic, C. Raman, D. Ray, D. A. Reis, M. Trigo, J. L. White, W. White, R. Wilcox, L. Young, R. N. Coffee, and P. H. Bucksbaum, "Time-resolved pump-probe experiments at the LCLS," Opt. Express **18**(17), 17620 (2010).
5. M. Csatari Divall, M. Kaiser, S. Hunziker, C. Vicario, B. Beutner, T. Schietinger, M. Lüthi, M. Pedrozzi, and C. Hauri, "Timing jitter studies of the SwissFEL Test Injector drive laser," Nucl. Instrum. Methods Phys. Res., Sect. A **735**, 471–479 (2014).

Optics EXPRESS

6. T. Katayama, S. Owada, T. Togashi, K. Ogawa, P. Karvinen, I. Vartiainen, A. Eronen, C. David, T. Sato, K. Nakajima, Y. Joti, H. Yumoto, H. Ohashi, and M. Yabashi, "A beam branching method for timing and spectral characterization of hard X-ray free-electron lasers," Struct. Dyn. **3**(3), 034301 (2016).
7. H. Kang, C. Min, H. Heo, C. Kim, H. Yang, G. Kim, I. Nam, S. Baek, H. Choi, G. Mun, B. Park, Y. Suh, D. Shin, J. Hu, J. Hong, S. Jung, S. Kim, K. Kim, D. Na, S. Park, Y. Park, J. Han, Y. Jung, S. Jeong, H. Lee, S. Lee, S. Lee, W. Lee, B. Oh, H. Suh, Y. Parc, S. Park, M. Kim, N. Jung, Y. Kim, M. Lee, B. Lee, C. Sung, I. Mok, J. Yang, C. Lee, H. Shin, J. Kim, Y. Kim, J. Lee, S. Park, J. Kim, J. Park, I. Eom, S. Rah, S. Kim, K. Nam, J. Park, J. Park, S. Kim, S. Kwon, S. Park, K. Kim, H. Hyun, S. Kim, S. Kim, S. Hwang, M. Kim, C. Lim, C. Yu, B. Kim, T. Kang, K. Kim, S. Kim, H. Lee, H. Lee, K. Park, T. Koo, D. Kim, and I. Ko, "Hard X-ray free-electron laser with femtosecond-scale timing jitter," Nat. Photonics **11**(11), 708–713 (2017).
8. H. Kirkwood, R. Letrun, T. Tanikawa, J. Liu, M. Nakatsutsumi, M. Emons, T. Jezynski, G. Palmer, M. Lederer, R. Bean, J. Buck, S. Di Dio Cafisio, R. Graceffa, J. Grünert, S. Göde, H. Höppner, Y. Kim, Z. Konopkova, G. Mills, M. Makita, A. Pelka, T. Preston, M. Sikorski, C. Takem, K. Giewekemeyer, M. Chollet, P. Vagovic, H. Chapman, A. Mancuso, and T. Sato, "Initial observations of the femtosecond timing jitter at the European XFEL," Opt. Lett. **44**(7), 1650 (2019).
9. T. Sato, R. Letrun, H. Kirkwood, J. Liu, P. Vagovič, G. Mills, Y. Kim, C. Takem, M. Planas, M. Emons, T. Jezynski, G. Palmer, M. Lederer, S. Schulz, J. Mueller, H. Schlarb, A. Silenzi, G. Giovanetti, A. Parenti, M. Bergemann, T. Michelat, J. Szuba, J. Grünert, H. Chapman, and A. Mancuso, "Femtosecond timing synchronization at megahertz repetition rates for an x-ray free-electron laser," Optica **7**(6), 716 (2020).
10. S. Schulz, I. Grguraš, C. Behrens, H. Bromberger, J. T. Costello, M. K. Czwalinna, M. Felber, M. C. Hoffmann, M. Ilchen, H. Y. Liu, T. Mazza, M. Meyer, S. Pfeiffer, P. Prędki, S. Schefer, C. Schmidt, U. Wegner, H. Schlarb, and A. L. Cavalieri, "Femtosecond all-optical synchronization of an X-ray free-electron laser," Nat. Commun. **6**(1), 5938 (2015).
11. E. Saldin, E. Schneidmiller, Y. Shvyd'ko, and M. Yurkov, "X-ray FEL with a meV bandwidth," Nucl. Instrum. Methods Phys. Res., Sect. A **475**(1-3), 357–362 (2001).
12. A. L. Cavalieri, D. M. Fritz, S. H. Lee, P. H. Bucksbaum, D. A. Reis, J. Rudati, D. M. Mills, P. H. Fuoss, G. B. Stephenson, C. C. Kao, D. P. Siddons, D. P. Lowney, A. G. MacPhee, D. Weinstein, R. W. Falcone, R. Pahl, J. Als-Nielsen, C. Blome, S. Düsterer, R. Ischebeck, H. Schlarb, H. Schulte-Schrepping, T. Tschentscher, J. Schneider, O. Hignette, F. Sette, K. Sokolowski-Tinten, H. N. Chapman, R. W. Lee, T. N. Hansen, O. Synnergren, J. Larsson, S. Techert, J. Sheppard, J. S. Wark, M. Bergh, C. Caleman, G. Huldt, D. van der Spoel, N. Timneanu, J. Hajdu, R. A. Akre, E. Bong, P. Emma, P. Krejcik, J. Arthur, S. Brennan, K. J. Gaffney, A. M. Lindenberg, K. Luening, and J. B. Hastings, "Clocking Femtosecond X Rays," Phys. Rev. Lett. **94**(11), 114801 (2005).
13. E. L. Saldin, E. A. Schneidmiller, and M. V. Yurkov, "Statistical and coherence properties of radiation from x-ray free-electron lasers," New J. Phys. **12**(3), 035010 (2010).
14. T. Maltezopoulos, S. Cunovic, M. Wieland, M. Beye, A. Azima, H. Redlin, M. Krikunova, R. Kalms, U. Frühling, F. Budzyn, W. Wurth, A. Föhlisch, and M. Drescher, "Single-shot timing measurement of extreme-ultraviolet free-electron laser pulses," New J. Phys. **10**(3), 033026 (2008).
15. C. Gahl, A. Azima, M. Beye, M. Deppe, K. Döbrich, U. Hasslinger, F. Hennies, A. Melnikov, M. Nagasono, A. Pietzsch, M. Wolf, W. Wurth, and A. Föhlisch, "A femtosecond X-ray/optical cross-correlator," Nat. Photonics **2**(3), 165–169 (2008).
16. M. Bionta, H. Lemke, J. Cryan, J. Glownia, C. Bostedt, M. Cammarata, J.-C. Castagna, Y. Ding, D. Fritz, A. R. Fry, J. Krzywinski, M. Messerschmidt, S. Schorb, M. Swiggers, and R. Coffee, "Spectral encoding of x-ray/optical relative delay," Opt. Express **19**(22), 21855 (2011).
17. F. Tavella, N. Stojanovic, G. Geloni, and M. Gensch, "Few-femtosecond timing at fourth-generation X-ray light sources," Nat. Photonics **5**(3), 162–165 (2011).
18. M. Harmand, R. Coffee, M. R. Bionta, M. Chollet, D. French, D. Zhu, D. M. Fritz, H. T. Lemke, N. Medvedev, B. Ziaja, S. Toleikis, and M. Cammarata, "Achieving few-femtosecond time-sorting at hard X-ray free-electron lasers," Nat. Photonics **7**(3), 215–218 (2013).
19. R. Riedel, A. Al-Shemmary, M. Gensch, T. Golz, M. Harmand, N. Medvedev, M. J. Prandolini, K. Sokolowski-Tinten, S. Toleikis, U. Wegner, B. Ziaja, N. Stojanovic, and F. Tavella, "Single-shot pulse duration monitor for extreme ultraviolet and X-ray free-electron lasers," Nat. Commun. **4**(1), 1731 (2013).
20. S. Eckert, M. Beye, A. Pietzsch, W. Quevedo, M. Hantschmann, M. Ochmann, M. Ross, M. P. Minitti, J. J. Turner, S. P. Moeller, W. F. Schlotter, G. L. Dakovski, M. Khalil, N. Huse, and A. Föhlisch, "Principles of femtosecond X-ray/optical cross-correlation with X-ray induced transient optical reflectivity in solids," Appl. Phys. Lett. **106**(6), 061104 (2015).
21. M. Csatari Divall, P. Mutter, E. Divall, and C. Hauri, "Femtosecond resolution timing jitter correction on a TW scale Ti:sapphire laser system for FEL pump-probe experiments," Opt. Express **23**(23), 29929 (2015).
22. E. Savelyev, R. Boll, C. Bomme, N. Schirmel, H. Redlin, B. Erk, S. Düsterer, E. Müller, H. Höppner, S. Toleikis, J. Müller, M. Kristin Czwalinna, R. Treusch, T. Kierspel, T. Mullins, S. Trippel, J. Wiese, J. Küpper, F. Braße, F. Krecinic, A. Rouzée, P. Rudawski, P. Johnsson, K. Amini, A. Lauer, M. Burt, M. Brouard, L. Christensen, J. Thøgersen, H. Stapelfeldt, N. Berrah, M. Müller, A. Ulmer, S. Techert, A. Rudenko, and D. Rolles, "Jitter-correction for IR/UV-XUV pump-probe experiments at the FLASH free-electron laser," New J. Phys. **19**(4), 043009 (2017).

Optics EXPRESS

23. S. Owada, K. Nakajima, T. Togashi, T. Kayatama, and M. Yabashi, "Single-shot arrival timing diagnostics for a soft X-ray free-electron laser beamline at SACLA," J. Synchrotron Radiat. **25**(1), 68–71 (2018).
24. M. Xin, K. Şafak, and F. Kärtner, "Ultra-precise timing and synchronization for large-scale scientific instruments," Optica **5**(12), 1564 (2018).
25. N. Hartmann, W. Helml, A. Galler, M. R. Bionta, J. Grünert, S. L. Molodtsov, K. R. Ferguson, S. Schorb, M. L. Swiggers, S. Carron, C. Bostedt, J.-C. Castagna, J. Bozek, J. M. Glownia, D. J. Kane, A. R. Fry, W. E. White, C. P. Hauri, T. Feurer, and R. N. Coffee, "Sub-femtosecond precision measurement of relative X-ray arrival time for free-electron lasers," Nat. Photonics **8**(9), 706–709 (2014).
26. E. Allaria, R. Appio, L. Badano, W. Barletta, S. Bassanese, S. Biedron, A. Borga, E. Busetto, D. Castronovo, P. Cinquegrana, S. Cleva, D. Cocco, M. Cornacchia, P. Craievich, I. Cudin, G. D'Auria, M. Dal Forno, M. Danailov, R. De Monte, G. De Ninno, P. Delgiusto, A. Demidovich, S. Di Mitri, B. Diviacco, A. Fabris, R. Fabris, W. Fawley, M. Ferianis, E. Ferrari, S. Ferry, L. Froehlich, P. Furlan, G. Gaio, F. Gelmetti, L. Giannessi, M. Giannini, R. Gobessi, R. Ivanov, E. Karantzoulis, M. Lonza, A. Lutman, B. Mahieu, M. Milloch, S. Milton, M. Musardo, I. Nikolov, S. Noe, F. Parmigiani, G. Penco, M. Petronio, L. Pivetta, M. Predonzani, F. Rossi, L. Rumiz, A. Salom, C. Scafuri, C. Serpico, P. Sigalotti, S. Spampinati, C. Spezzani, M. Svandrlik, C. Svetina, S. Tazzari, M. Trovo, R. Umer, A. Vascotto, M. Veronese, R. Visintini, M. Zaccaria, D. Zangrando, and M. Zangrando, "Highly coherent and stable pulses from the FERMI seeded free-electron laser in the extreme ultraviolet," Nat. Photonics **6**(10), 699–704 (2012).
27. T. Tschentscher, C. Bressler, J. Grünert, A. Madsen, A. Mancuso, M. Meyer, A. Scherz, H. Sinn, and U. Zastrau, "Photon Beam Transport and Scientific Instruments at the European XFEL," Appl. Sci. **7**(6), 592 (2017).
28. W. Decking, S. Abeghyan, P. Abramian, A. Abramsky, A. Aguirre, C. Albrecht, P. Alou, M. Altarelli, P. Altmann, K. Amyan, V. Anashin, E. Apostolov, K. Appel, D. Auguste, V. Ayvazyan, S. Baark, F. Babies, N. Baboi, P. Bak, V. Balandin, R. Baldinger, B. Baranasic, S. Barbanotti, O. Belikov, V. Belokurov, L. Belova, V. Belyakov, S. Berry, M. Bertucci, B. Beutner, A. Block, M. Blöcher, T. Böckmann, C. Bohm, M. Böhnert, V. Bondar, E. Bondarchuk, M. Bonezzi, P. Borowiec, C. Bösch, U. Bösenberg, A. Bosotti, R. Böspflug, M. Bousonville, E. Boyd, Y. Bozhko, A. Brand, J. Branlard, S. Briechle, F. Brinker, S. Brinker, R. Brinkmann, S. Brockhauser, O. Brovko, H. Brück, A. Brüdgam, L. Butkowski, T. Büttner, J. Calero, E. Castro-Carballo, G. Cattalanotto, J. Charrier, J. Chen, A. Cherepenko, V. Cheskidov, M. Chiodini, A. Chong, S. Choroba, M. Chorowski, D. Churanov, W. Cichalewski, M. Clausen, W. Clement, C. Cloué, J. A. Cobos, N. Coppola, S. Cunis, K. Czuba, M. Czwalinna, B. D'Almagne, J. Dammann, H. Danared, A. de Zubiaurre Wagner, A. Delfs, T. Delfs, F. Dietrich, T. Dietrich, M. Dohlus, M. Dommach, A. Donat, X. Dong, N. Doynikov, M. Dressel, M. Duda, P. Duda, H. Eckoldt, W. Ehsan, J. Eidam, F. Eints, C. Engling, U. Englisch, A. Ermakov, K. Escherich, J. Eschke, E. Saldin, M. Faesing, A. Fallou, M. Felber, M. Fenner, B. Fernandes, J. M. Fernández, S. Feuker, K. Filippakopoulos, K. Floettmann, V. Fogel, M. Fontaine, A. Francés, I. F. Martin, W. Freund, T. Freyermuth, M. Friedland, L. Fröhlich, M. Fusetti, J. Fydrych, A. Gallas, O. García, L. Garcia-Tabares, G. Geloni, N. Gerasimova, C. Gerth, P. Geßler, V. Gharibyan, M. Gloor, J. Głowinkowski, A. Goessel, Z. Gołębiewski, N. Golubeva, W. Grabowski, W. Graeff, A. Grebentsov, M. Grecki, T. Grevsmuehl, M. Gross, U. Grosse-Wortmann, J. Grünert, S. Grunewald, P. Grzegory, G. Feng, H. Guler, G. Gusev, J. L. Gutierrez, L. Hagge, M. Hamberg, R. Hanneken, E. Harms, I. Hartl, A. Hauberg, S. Hauf, J. Hauschildt, J. Hauser, J. Havlicek, A. Hedqvist, N. Heidbrook, F. Hellberg, D. Henning, O. Hensler, T. Hermann, A. Hidvégi, M. Hierholzer, H. Hintz, F. Hoffmann, M. Hoffmann, M. Hoffmann, Y. Holler, M. Hüning, A. Ignatenko, M. Ilchen, A. Iluk, J. Iversen, J. Iversen, M. Izquierdo, L. Jachmann, N. Jardon, U. Jastrow, K. Jensch, J. Jensen, M. Jeżabek, M. Jidda, H. Jin, N. Johannson, R. Jonas, W. Kaabi, D. Kaefer, R. Kammering, H. Kapitza, S. Karabekyan, S. Karstensen, K. Kasprzak, V. Katalev, D. Keese, B. Keil, M. Kholopov, M. Killenberger, B. Kitaev, Y. Klimchenko, R. Klos, L. Knebel, A. Koch, M. Koepke, S. Köhler, W. Köhler, N. Kohlstrunk, Z. Konopkova, A. Konstantinov, W. Kook, W. Koprek, M. Körfer, O. Korth, A. Kosarev, K. Kosiński, D. Kostin, Y. Kot, A. Kotarba, T. Kozak, V. Kozak, R. Kramert, M. Krasilnikov, A. Krasnov, B. Krause, L. Kravchuk, O. Krebs, R. Kretschmer, J. Kreutzkamp, O. Kröplin, K. Krzysik, G. Kube, H. Kuehn, N. Kujala, V. Kulikov, V. Kuzminych, D. La Civita, M. Lacroix, T. Lamb, A. Lancetov, M. Larsson, D. Le Pinvidic, S. Lederer, T. Lensch, D. Lenz, A. Leuschner, F. Levenhagen, Y. Li, J. Liebing, L. Lilje, T. Limberg, D. Lipka, B. List, J. Liu, S. Liu, B. Lorbeer, J. Lorkiewicz, H. H. Lu, F. Ludwig, K. Machau, W. Maciocha, C. Madec, C. Magueur, C. Maiano, I. Maksimova, K. Malcher, T. Maltezopoulos, E. Mamoshkina, B. Manschwetus, F. Marcellini, G. Marinkovic, T. Martinez, H. Martirosyan, W. Maschmann, M. Maslov, A. Matheisen, U. Mavric, J. Meißner, K. Meissner, M. Messerschmidt, N. Meyners, G. Michalski, P. Michelato, N. Mildner, M. Moe, F. Moglia, C. Mohr, S. Mohr, W. Möller, M. Mommerz, L. Monaco, C. Montiel, M. Moretti, I. Morozov, P. Morozov, D. Mross, J. Mueller, C. Müller, J. Müller, K. Müller, J. Munilla, A. Münnich, V. Muratov, O. Napoly, B. Näser, N. Nefedov, R. Neumann, R. Neumann, N. Ngada, D. Noelle, F. Obier, I. Okunev, J. A. Oliver, M. Omet, A. Oppelt, A. Ottmar, M. Oublaid, C. Pagani, R. Paparella, V. Paramonov, C. Peitzmann, J. Penning, A. Perus, F. Peters, B. Petersen, A. Petrov, I. Petrov, S. Pfeiffer, J. Pflüger, S. Philipp, Y. Pienaud, P. Pierini, S. Pivovarov, M. Planas, E. Pławski, M. Pohl, J. Polinski, V. Popov, S. Prat, J. Prenting, G. Priebe, H. Pryschelski, K. Przygoda, E. Pyata, B. Racky, A. Rathjen, W. Ratuschni, S. Regnaud-Campderros, K. Rehlich, D. Reschke, C. Robson, J. Roever, M. Roggli, J. Rothenburg, E. Rusiński, R. Rybaniec, H. Sahling, M. Salmani, L. Samoylova, D. Sanzone, F. Saretzki, O. Sawlanski, J. Schaffran, H. Schlarb, M. Schlösser, V. Schlott, C. Schmidt, F. Schmidt-Foehre, M. Schmitz, M. Schmökel, T. Schnautz, E. Schneidmiller, M. Scholz, B. Schöneburg, J. Schultze, C. Schulz, A. Schwarz, J. Sekutowicz, D. Sellmann, E. Semenov, S. Serkez, D. Sertore, N. Shehzad, P. Shemarykin, L. Shi, M. Sienkiewicz, D. Sikora, M. Sikorski, A. Silenzi, C. Simon, W. Singer, X. Singer, H. Sinn, K. Sinram, N. Skvorodnev, P. Smirnow, T. Sommer, A. Sorokin, M. Stadler, M. Steckel, B.

Optics EXPRESS

Steffen, N. Steinhau-Kühl, F. Stephan, M. Stodulski, M. Stolper, A. Sulimov, R. Susen, J. Świerblewski, C. Sydlo, E. Syresin, V. Sytchev, J. Szuba, N. Tesch, J. Thie, A. Thiebault, K. Tiedtke, D. Tischhauser, J. Tolkiehn, S. Tomin, F. Tonisch, F. Toral, I. Torbin, A. Trapp, D. Treyer, G. Trowitzsch, T. Trublet, T. Tschentscher, F. Ullrich, M. Vannoni, P. Varela, G. Varghese, G. Vashchenko, M. Vasic, C. Vazquez-Velez, A. Verguet, S. Vilcins-Czvitkovits, R. Villanueva, B. Visentin, M. Viti, E. Vogel, E. Volobuev, R. Wagner, N. Walker, T. Wamsat, H. Weddig, G. Weichert, H. Weise, R. Wenndorf, M. Werner, R. Wichmann, C. Wiebers, M. Wiencek, T. Wilksen, I. Will, L. Winkelmann, M. Winkowski, K. Wittenburg, A. Witzig, P. Wlk, T. Wohlenberg, M. Wojciechowski, F. Wolff-Fabris, G. Wrochna, K. Wrona, M. Yakopov, B. Yang, F. Yang, M. Yurkov, I. Zagorodnov, P. Zalden, A. Zavadtsev, D. Zavadtsev, A. Zhirnov, A. Zhukov, V. Ziemann, A. Zolotov, N. Zolotukhina, F. Zummack, and D. Zybin, "A MHz-repetition-rate hard X-ray free-electron laser driven by a superconducting linear accelerator," Nat. Photonics **14**(6), 391–397 (2020).

29. M. Bionta, N. Hartmann, M. Weaver, D. French, D. Nicholson, J. Cryan, J. Glownia, K. Baker, C. Bostedt, M. Chollet, Y. Ding, D. Fritz, A. Fry, D. Kane, J. Krzywinski, H. Lemke, M. Messerschmidt, S. Schorb, D. Zhu, W. White, and R. Coffee, "Spectral encoding method for measuring the relative arrival time between x-ray/optical pulses," Rev. Sci. Instrum. **85**(8), 083116 (2014).
30. J. Liu, F. Dietrich, and J. Grünert, "Photon Arrival Time Monitor (PAM) at the European XFEL," Tech. rep., European XFEL GmbH (2017).
31. S. Düsterer, P. Radcliffe, C. Bostedt, J. Bozek, A. L. Cavalieri, R. Coffee, J. T. Costello, D. Cubaynes, L. F. DiMauro, Y. Ding, G. Doumy, F. Grüner, W. Helml, W. Schweinberger, R. Kienberger, A. R. Maier, M. Messerschmidt, V. Richardson, C. Roedig, T. Tschentscher, and M. Meyer, "Femtosecond x-ray pulse length characterization at the Linac Coherent Light Source free-electron laser," New J. Phys. **13**(9), 093024 (2011).
32. W. Helml, I. Grguraš, P. Juranić, S. Düsterer, T. Mazza, A. Maier, N. Hartmann, M. Ilchen, G. Hartmann, L. Patthey, C. Callegari, J. Costello, M. Meyer, R. Coffee, A. Cavalieri, and R. Kienberger, "Ultrashort Free-Electron Laser X-ray Pulses," Appl. Sci. **7**(9), 915 (2017).
33. G. Kastirke, M. Schöffler, M. Weller, J. Rist, R. Boll, N. Anders, T. Baumann, S. Eckart, B. Erk, A. De Fanis, K. Fehre, A. Gatton, S. Grundmann, P. Grychtol, A. Hartung, M. Hofmann, M. Ilchen, C. Janke, M. Kircher, M. Kunitski, X. Li, T. Mazza, N. Melzer, J. Montano, V. Music, G. Nalin, Y. Ovcharenko, A. Pier, N. Rennhack, D. Rivas, R. Dörner, D. Rolles, A. Rudenko, P. Schmidt, J. Siebert, N. Strenger, D. Trabert, I. Vela-Perez, R. Wagner, T. Weber, J. Williams, P. Ziolkowski, L. Schmidt, A. Czasch, K. Ueda, F. Trinter, M. Meyer, P. Demekhin, and T. Jahnke, "Double Core-Hole Generation in O2 Molecules Using an X-Ray Free-Electron Laser: Molecular-Frame Photoelectron Angular Distr," Phys. Rev. Lett. **125**(16), 163201 (2020).
34. U. Eichmann, H. Rottke, S. Meise, M. Meyer, T. M. Baumann, R. Boll, A. D. Fanis, P. Grychtol, M. Ilchen, T. Mazza, J. Montano, V. Music, Y. Ovcharenko, D. E. Rivas, S. Serkez, R. Wagner, and S. Eisebitt, "Photon-recoil imaging: Expanding the view of nonlinear x-ray physics," Science **369**(6511), 1630–1633 (2020).
35. G. Kastirke, M. Schöffler, M. Weller, J. Rist, R. Boll, N. Anders, T. Baumann, S. Eckart, B. Erk, A. Fanis, K. Fehre, A. Gatton, S. Grundmann, P. Grychtol, A. Hartung, M. Hofmann, M. Ilchen, C. Janke, M. Kircher, M. Kunitski, X. Li, T. Mazza, N. Melzer, J. Montano, V. Music, G. Nalin, Y. Ovcharenko, A. Pier, N. Rennhack, D. Rivas, R. Dörner, D. Rolles, A. Rudenko, P. Schmidt, J. Siebert, N. Strenger, D. Trabert, I. Vela-perez, R. Wagner, T. Weber, J. Williams, P. Ziolkowski, L. Schmidt, A. Czasch, F. Trinter, M. Meyer, and K. Ueda, "Photoelectron Diffraction Imaging of a Molecular Breakup Using an X-Ray Free-Electron Laser," Phys. Rev. X **10**(2), 021052 (2020).
36. T. Mazza, M. Ilchen, M. Kiselev, E. Gryzlova, T. Baumann, R. Boll, A. D. Fanis, P. Grychtol, J. Montaño, V. Music, Y. Ovcharenko, N. Rennhack, D. Rivas, P. Schmidt, R. Wagner, P. Ziolkowski, N. Berrah, B. Erk, P. Johnsson, L. Marder, M. Martins, C. Ott, S. Pathak, T. Pfeifer, D. Rolles, O. Zatsarinny, and M. Meyer, "Mapping Resonance Structures in Transient Core-Ionized Atoms," Phys. Rev. X **10**(4), 041056 (2020).
37. T. Jahnke, R. Guillemin, L. Inhester, S.-K. Son, G. Kastirke, M. Ilchen, J. Rist, D. Trabert, N. Melzer, N. Anders, T. Mazza, R. Boll, A. De Fanis, V. Music, T. Weber, M. Weller, S. Eckart, K. Fehre, S. Grundmann, A. Hartung, M. Hofmann, C. Janke, M. Kircher, G. Nalin, A. Pier, J. Siebert, N. Strenger, I. Vela-Perez, T. Baumann, P. Grychtol, J. Montano, Y. Ovcharenko, N. Rennhack, D. Rivas, R. Wagner, P. Ziolkowski, P. Schmidt, T. Marchenko, O. Travnikova, L. Journel, I. Ismail, E. Kukk, J. Niskanen, F. Trinter, C. Vozzi, M. Devetta, S. Stagira, M. Gisselbrecht, A. Jäger, X. Li, Y. Malakar, M. Martins, R. Feifel, L. Schmidt, A. Czasch, G. Sansone, D. Rolles, A. Rudenko, R. Moshammer, R. Dörner, M. Meyer, T. Pfeiffer, M. Schüffler, R. Santra, N. Simon, and M. Piancastelli, "Inner-shell-ionization-induced femtosecond structural dynamics of water molecules imaged at an x-ray free-electron laser," *Phys. Rev. X* accepted (2020).
38. J. Müller, M. Felber, T. Kozak, T. Lamb, S. Schulz, C. Sydlo, M. Titberidze, F. Zummack, and H. Schlarb, "Large-scale optical synchronization system of the European XFEL," in *Proc. 29th Linear Accelerator Conference (LINAC'18)*, (JACoW Publishing, 2019), pp. 253–256.
39. R. Letrun, "private communications," research article **in preparation** (2021).
40. H. Dinter, "Longitudinal Diagnostics for Beam-Based Intra Bunch-Train Feedback at FLASH and the European XFEL," Ph.D. thesis, University Hamburg (2018).
41. M. Krause, F. Stevie, L. Lewis, T. Carlson, and W. Moddeman, "Multiple excitation of neon by photon and electron impact," Phys. Lett. A **31**(2), 81–82 (1970).
42. J. Schins, P. Breger, P. Agostini, R. Constantinescu, H. Muller, G. Grillon, A. Antonetti, and A. Mysyrowicz, "Observation of Laser-Assisted Auger Decay in Argon," Phys. Rev. Lett. **73**(16), 2180–2183 (1994).

Optics EXPRESS

43. A. Kazansky and N. Kabachnik, "On the gross structure of sidebands in the spectra of laser-assisted Auger decay," J. Phys. B: At. Mol. Opt. Phys. **43**(3), 035601 (2010).
44. A. K. Kazansky, I. P. Sazhina, and N. M. Kabachnik, "Angle-resolved electron spectra in short-pulse two-color XUV + IR photoionization of atoms," Phys. Rev. A **82**(3), 033420 (2010).
45. M. Meyer, P. Radcliffe, T. Tschentscher, J. T. Costello, A. L. Cavalieri, I. Grguras, A. R. Maier, R. Kienberger, J. Bozek, C. Bostedt, S. Schorb, R. Coffee, M. Messerschmidt, C. Roedig, E. Sistrunk, L. F. Di Mauro, G. Doumy, K. Ueda, S. Wada, S. Düsterer, A. K. Kazansky, and N. M. Kabachnik, "Angle-Resolved Electron Spectroscopy of Laser-Assisted Auger Decay Induced by a Few-Femtosecond X-Ray Pulse," Phys. Rev. Lett. **108**(6), 063007 (2012).
46. A. De Fanis, "private communications," research article, submitted (2021).
47. P. Finetti, H. Höppner, E. Allaria, C. Callegari, F. Capotondi, P. Cinquegrana, M. Coreno, R. Cucini, M. Danailov, A. Demidovich, G. Ninno, M. Fraia, R. Feifel, E. Ferrari, L. Fröhlich, D. Gauthier, T. Golz, C. Grazioli, Y. Kai, G. Kurdi, N. Mahne, M. Manfredda, N. Medvedev, I. Nikolov, E. Pedersoli, G. Penco, O. Plekan, M. Prandolini, K. Prince, L. Raimondi, P. Rebernik, R. Riedel, E. Roussel, P. Sigalotti, R. Squibb, N. Stojanovic, S. Stranges, C. Svetina, T. Tanikawa, U. Teubner, V. Tkachenko, S. Toleikis, M. Zangrando, B. Ziaja, F. Tavella, and L. Giannessi, "Pulse duration of seeded free-electron lasers," Phys. Rev. X **7**(2), 021043 (2017).
48. A. K. Kazansky, I. P. Sazhina, and N. M. Kabachnik, "Time-dependent theory of Auger decay induced by ultra-short pulses in a strong laser field," J. Phys. B: At. Mol. Opt. Phys. **42**(24), 245601 (2009).
49. D. Dahl, "SIMION for the personal computer in reflection," Int. J. Mass Spectrom. **200**(1-3), 3–25 (2000).
50. F. Löhl, V. Arsov, M. Felber, K. Hacker, W. Jalmuzna, B. Lorbeer, F. Ludwig, K.-H. Matthiesen, H. Schlarb, B. Schmidt, P. Schmüser, S. Schulz, J. Szewinski, A. Winter, and J. Zemella, "Electron Bunch Timing with Femtosecond Precision in a Superconducting Free-Electron Laser," Phys. Rev. Lett. **104**(14), 144801 (2010).
51. M. Viti, M. Czwalinna, H. Dinter, C. Gerth, K. Przygoda, R. Rybaniec, and H. Schlarb, "The Bunch Arrival Time Monitor At Flash and European Xfel," in *16th Int. Conf. on Accelerator and Large Experimental Control Systems*, (2017), pp. 701–705.
52. M. Pergament, G. Palmer, M. Kellert, K. Kruse, J. Wang, L. Wissmann, U. Wegner, M. Emons, D. Kane, G. Priebe, S. Venkatesan, T. Jezynski, F. Pallas, and M. J. Lederer, "Versatile optical laser system for experiments at the European X-ray free-electron laser facility," Opt. Express **24**(26), 29349 (2016).
53. G. Palmer, M. Kellert, J. Wang, M. Emons, U. Wegner, D. Kane, F. Pallas, T. Jezynski, S. Venkatesan, D. Rompotis, E. Brambrink, B. Monoszlai, M. Jiang, J. Meier, K. Kruse, M. Pergament, and M. Lederer, "Pump-probe laser system at the FXE and SPB/SFX instruments of the European X-ray Free-Electron Laser Facility," J. Synchrotron Radiat. **26**(2), 328–332 (2019).
54. D. Rivas, "Commissioning SQS Laser," European XFEL (2019), https://doi.org/10.22003/XFEL.EU-DATA-002556-00.